Research Article

COMPUTATIONAL MODELING OF COLD FLOW CHARACTERISTICS OF A SINGLE CYLINDER INTERNAL COMBUSTION ENGINE FOR DIFFERENT TURBULENCE MODELS

İsmail Hakkı Savcı[1], M. Zafer Gül[2]

[1] *Department of CAE, Ford Otosan, Istanbul, Turkey*
[2] *Department of Mechanical Engineering, Marmara University, Istanbul, Turkey*
isavci@ford.com.tr,zgul@marmara.edu.tr, 0000-0002-5943-7763

ABSTRACT

The recent developments of the CFD tools enable predicting the fluid dynamic, heat transfer, combustion, chemical reaction and spray formation process even in very complex geometries with a sufficient degree of accuracy and acceptable computational costs by numerical solutions of the governing conservation equations that have become a realizable goal. The principal components of these multidimensional engine flow models contain the mathematical models, the discretization procedures, and the solution algorithm. In addition, mathematical models or equations are used to describe the flow processes. Especially turbulence model, describing the small-scale features of the flow, is essential. The dynamic mesh model in Star-CD can be used to model flows where the shape of the domain changes with time due to motion on the domain boundaries. The update of the volume mesh is handled automatically by Star-CD at each time step based on the new positions of the boundaries. To use the dynamic mesh model, you need to provide a starting volume mesh and describe the motion as valve profile of any moving zones in the model. A simplified 3D geometry (from Imperial College compressing engine) will be used for this work, consisting of a simple compressor geometry, the bottom wall representing the piston. The simulation will be performed in an axisymmetric geometry from the TDC position (i.e., CA =0 0) to the end of the compression stroke (i.e., CA=3600). The development of CFD methodology for IC engine design represents a particular challenge due to the complex physics and mechanics. Turbulence modeling is one of the critical parameters for ICE CFD applications. Standard k-□ model has been widely used for the CFD calculation for the IC engine applications, other turbulence models are used as k-□-□ model (Gul extended a three-equation model) that can have a better account for compression and expansion effects. The main task of this project is to provide a numerical simulation of the intake flow field

and axis-symmetric cylinder. Two- dimensional computational analyses were performed on the axis-symmetric cylinder with k-□-□ and k-□ turbulence model. Results of the two-dimensional analysis were compared the numerical results to the flow field measurement.

Keywords: *ICE, CFD, Turbulence, cylinder*

1. INTRODUCTION

Multi-dimensional CFD analysis is important especially in the case of simulation of the cylinder since the design in unconventional. Multi-dimensional analysis can provide valuable information in comparing the flow fields of the axisymmetry [1]. Two-dimensional computational fluid dynamic analysis was performed on the axissymetry valve engine using STAR-CD [2]. Modern commercial CFD tools like STAR-CD offer more complex tools like turbulence modeling, dynamic mesh modification etc. which could be utilized for simulation. Also visualization tools as En-sight and STAR-CD can be used to plot and understand the flow features more effectively [3-5].

Two-dimensional analysis allows us to model the system in more detail without having the computational cost and effort of a three-dimensional analysis. It is important to capture the 2D effects of flow through the valve in order to study the local effects such as recirculation, swirl etc. [6-9].

In this study, two sets of simulations were performed for part load at 200 RPM with different compression ratios 3.5, 6.7 respectively with same valve profile. Multi-dimensional engine modeling method was built and developed to calculate of fluid flow in an idealized version of axisymmetric engine. Turbulent flow in-cylinder was considered. For the fluid flow, standard k-ε turbulence model and RNG k-ε turbulence model are utilized. Several cycles were run and convergence was monitored based on the mass balance inside the cylinder.

The in-cylinder flow in axisymmetric geometries and the flow through the inlet valve for unsteady conditions are investigated and experimental results are presented. The governing equations subject to relevant boundary conditions were solved numerically using finite-volume method. The upwind technique was employed to discretize the convective terms. PISO algorithm was used.

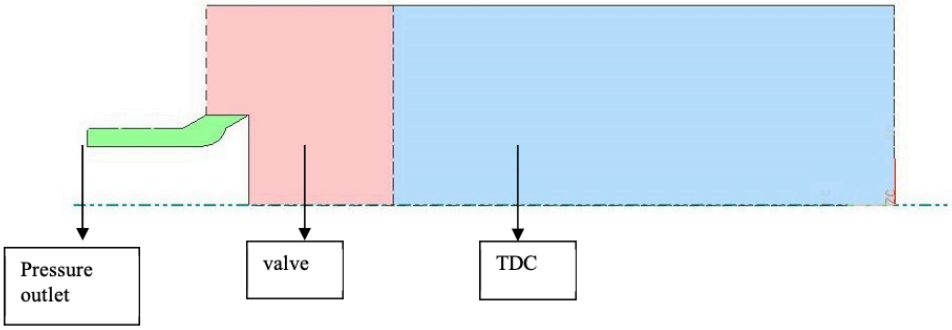

Figure 1. Geometry of the Case I

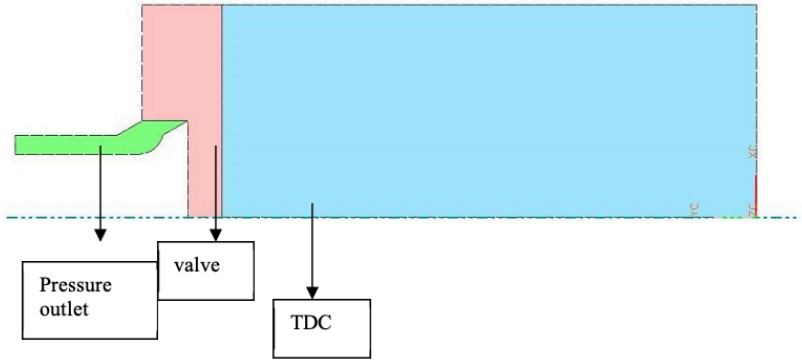

Figure 2. Geometry of the Case II

2. COMPUTATIONAL MODELLING

The computer code STARCD was used to model the intake system in axisymmetry engine. The configuration of the cylinder with its ports is shown in Fig. 3.The engine parameters used in this study are listed in Table 1. The engine had a bore of 75 mm and a stroke of 94 mm.

The cylinder is axisymmetric and exhaust valves are located at the cylinder axis. In order to obtain flow field and combustion characteristics, the ensemble-averaged differential form of continuity, momentum, enthalpy and standard k-ε equations are solved with appropriate boundary conditions [10-12].

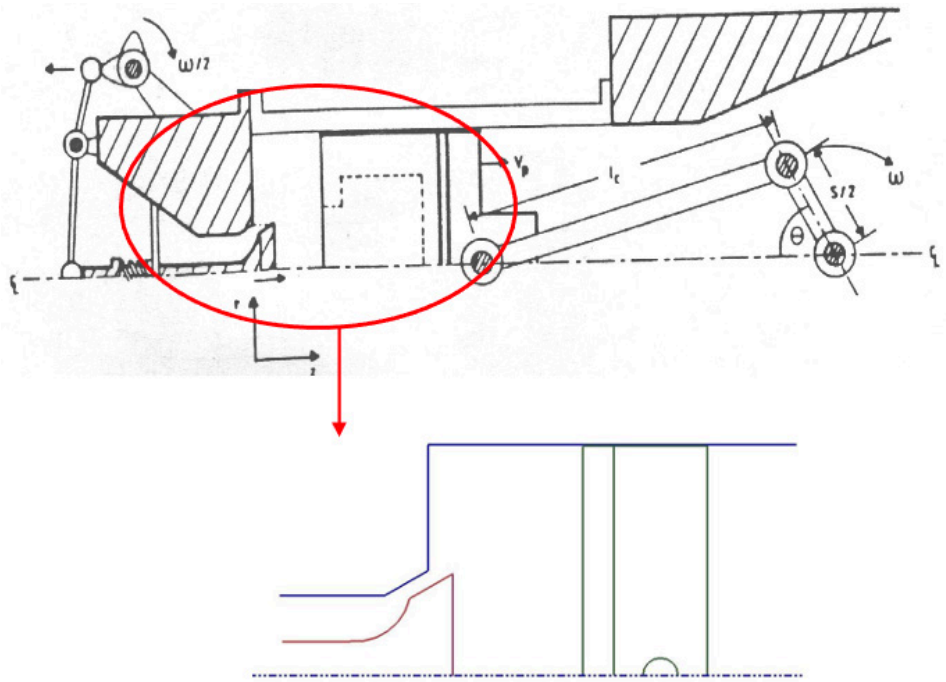

Figure 3. Diagram of Imperial College Compressing Engine Simulator

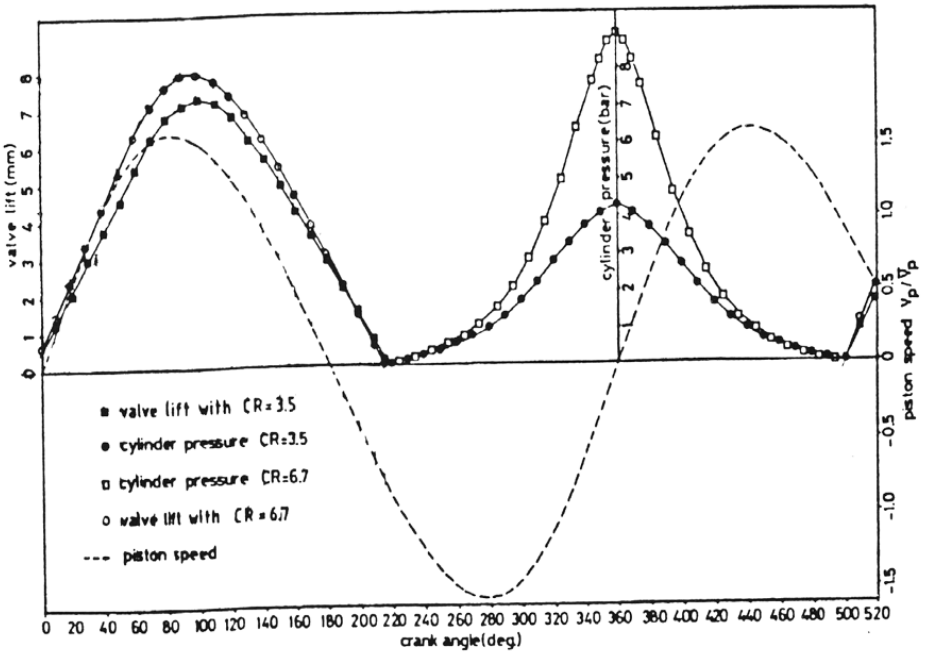

Figure 4. Variation of Valve Lift, Piston Speed and Cylinder Pressure with Crank Angle of the Model Engines

The simulations were performed through the intake and compression strokes only. The exhaust system in this engine was not modeled since the exhaust valves were not considered to open. Details of the computational mesh are shown in Figure . The mesh had about 380,000 cells. Pressure inflow boundaries were imposed at the open ends of the intake runners. The calculations were started at a crank angle of 345 degrees (15 degrees before TDC the beginning of the intake stroke). The air, in the cylinder was considered to be quiescent at the beginning of the simulation.

Table 1. Details of Test Cases; the Imperial College 2D Engine Simulator

	Case I	**Case II**
Cylinder Bore (mm)	75	75
Stroke (mm)	94	94
Connecting-Rod Length (mm)	363.5	363.5
Compression Ratio	3.5	6.7
Engine Speed (rpm)	200	200
Mean Piston Velocity (m/s)	0.626667	0.626667
Max. Valve Lift (L_{max}) (mm)	7.3	8
Valve Diameter (D_V) (mm)	34	34
L_{max}/D_V	0.21	0.24
Valve seat angle	60^o	60^o

Two different cases are simulated. Table 1 lists these cases with a description of each cases.

At the beginning of the computation the inlet and initial values of variables, including mass flow rate, radial and axial velocity components, must be specified. The computation started at TDC and the initial velocity assumed as zero. However, to decrease the uncertainties the results were evaluated after one complete cycle run (i.e. after 360o). Details of operating conditions are in the Table 2.

Table 2. Valve Opening and Closing and Estimated Temperatures of the Engine Simulator

	Case I	**Case II**
Valve opening for intake	-6° CA	-6° CA
Valve closing for intake	226° CA	226° CA
Valve opening for exhaust	496° CA	496° CA
Valve closing for intake	6° CA	6° CA
Cylinder Wall Temp (K)	340	350
Cylinder Head & Wall (K	340	350
Piston (K)	360	370

Star-CD uses PISO algorithm for transient flow solution. The simulation was run over 360 time steps of 0.5 ca each, hence covering the opens cycle. This time step led to average Courant numbers within the mesh being in range 0.1 to 1. Typical runs took 2 days on HP-Unix machine. Post Processing information being written out for pressure, three components of velocity, turbulence intensity and density.

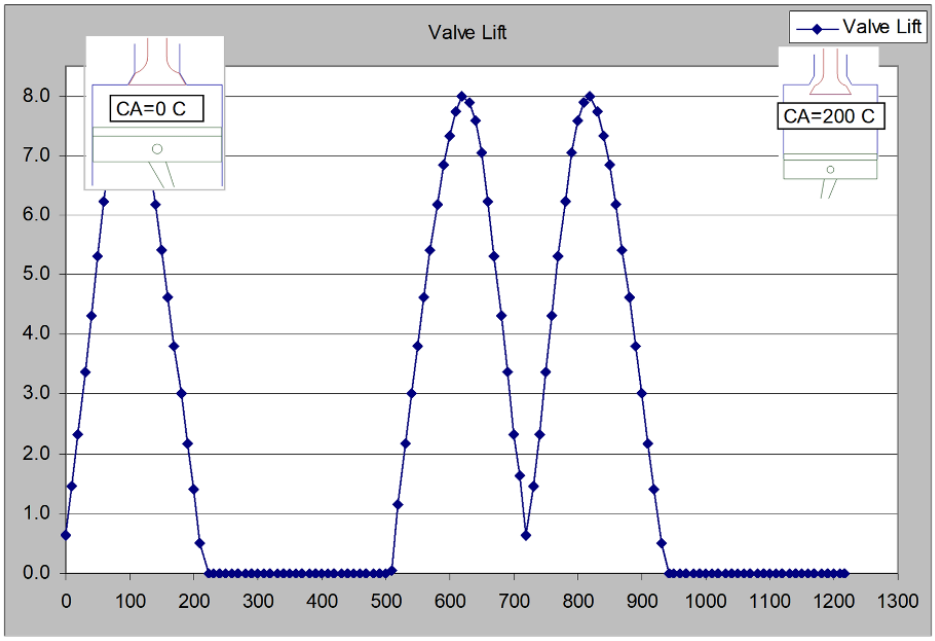

Figure 5. Valve Lift of the Engine Simulator

The simulations was commenced at 900C TDC. The cylinder was initiated to have zero velocity with a pressure and temperature of 109.3 kPa and 299 K respectively.

The cylinder pressure, species densities, turbulent kinetic energy and turbulence length scale are assumed to be uniform at the beginning of computation at the intake valve closure. The turbulent kinetic energy and dissipation rate within the cylinder and ducts were initialized at 1 m2/s2 and 1000 m2/s3 respectively, representing a relatively quiescent fluid with turbulent viscosity of close to 10-4 kg/s/m.

When the numerical solutions obtained on different grids agree to within a level of tolerance specified by the user, they are referred to as "grid converged" solutions. The concept of grid convergence applies to the finite-volume approach also where numerical solution, if correct, becomes independent of the grid as the cell reduced. It is very important that you investigate the effect of grid resolution on the solution in every CFD problem you solve. A CFD solution cannot be trusted unless you have convinced yourself that the solution is grid converged to an acceptance level of tolerance (which would be problem dependent) [13-15].

In order to obtain a solution independent of the grid distribution, grid sensitivity tests can be performed by tracing the cylinder pressure against crank angle. It is found that the solution becomes almost independent with uniform 250 grids in ξ direction and 150 uniform grids in the r-direction.

3. RESULTS AND DISCUSSION

In this study turbulent flow in an idealized homogeneous axissymetric engine are analyzed numerically. The valve is modeled so valve effects are taken into account. Computations are performed for different compression ratio r=3.7, r=6 respectively, with constant engine speed N=200 rpm, stroke L=0.09 m and ri= 0.04 m and rd=0.0567 m are chosen. Ideal gas is used to model compressible effects as a air.

For both test cases an overall impression of the in-cylinder behavior is provided in terms of plots at selected crank angles. All data shown in figures were obtained for 300000 grid-density run. The predictions of the standard k-e and RNG turbulence model was presented in figures. Computational grid arrangements for test Case I and Case II can be seen in the Figure 6.

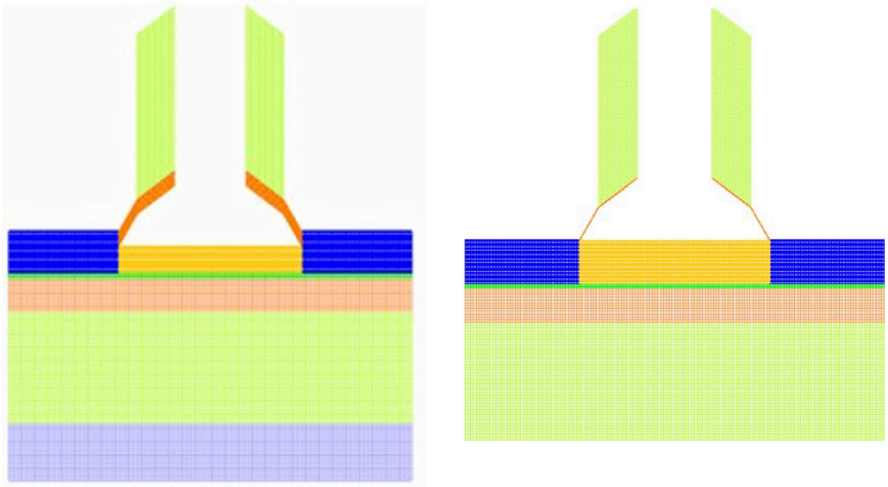

Figure 6. Computational grid arrangements; (CR= 3.5) □□ □ = 36^0 and 360^0

In Figure 7- Figure 8, the predictions of the velocity fields (velocity field and velocity magnitude) for test Case I are presented for both models. And, the turbulence intensity distributions for this test case are shown in Figure 9 & Figure 10.

The vector plots of velocity field for test Case II are shown in Figure 11 and 12 for both models.

The predictions of the axial mean velocity and turbulence intensity profiles of the standard k-□ and are compared with the experimental data in Figures 13 and Figures 14 for test Case I and Case II, respectively.

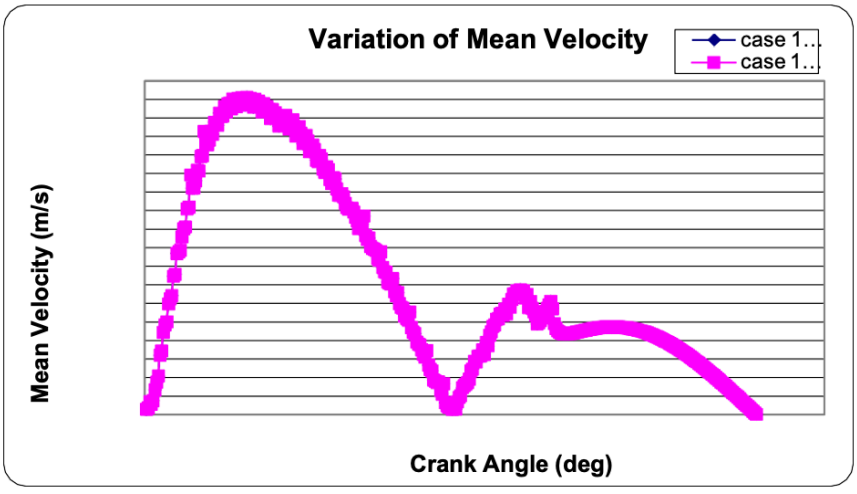

Figure 7. Variation of Mean Velocity of the case I

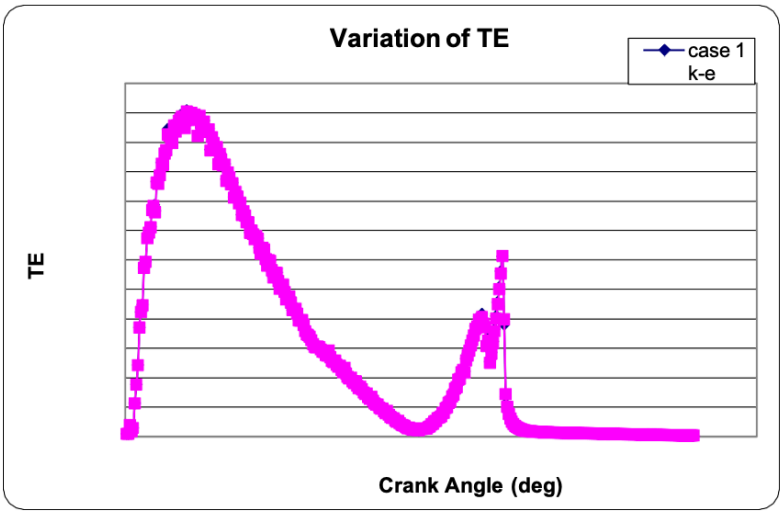

Figure 8. Variation of Turbulence Energy of the case I

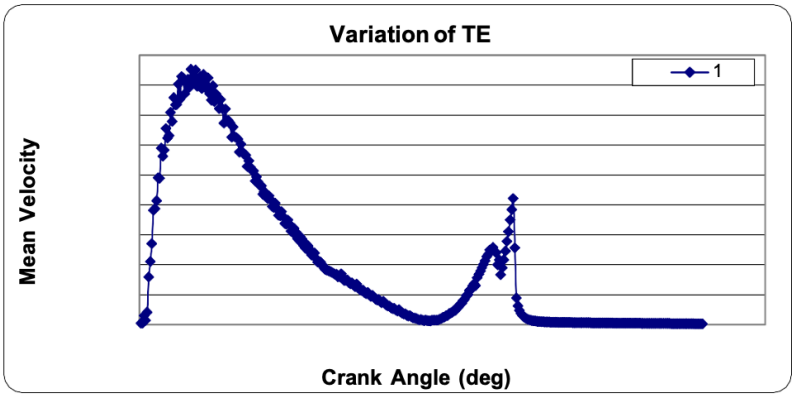

Figure 9. Variation of Turbulence Energy of the Case II

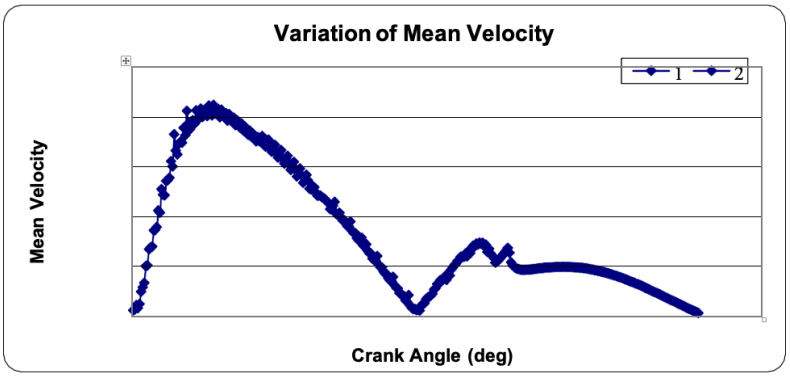

Figure 10. Variation of Mean Velocity of the Case II

4. THE PREDICTIONS AND COMPARISONS FOR CASE I

The flow field during early stages of induction (for □=360 to 900 CA) can be seen can be seen from Figure 11 & Figure 12. Although appearing to undergo minor deflections, intake flow penetrates and impinges on the piston or cylinder wall, depending on the piston position. Then, it separates into two strong recirculation zones (vortex) oneof which is formed at the cylinder head-wall corner and the other is formed behind the inlet valve. Both vortices are toroidal. The center of both recirculation zones appears to be slightly more to left than those of the k-□ model. The centers of both recirculation zones move downstream towards the piston until mid-intake stroke; this movement is small in the former while the latter stretches and becomes the dominant one. In the induction angular range (□=180) the swirl motion increases proportionally with the valve opening, apart from the late stage.

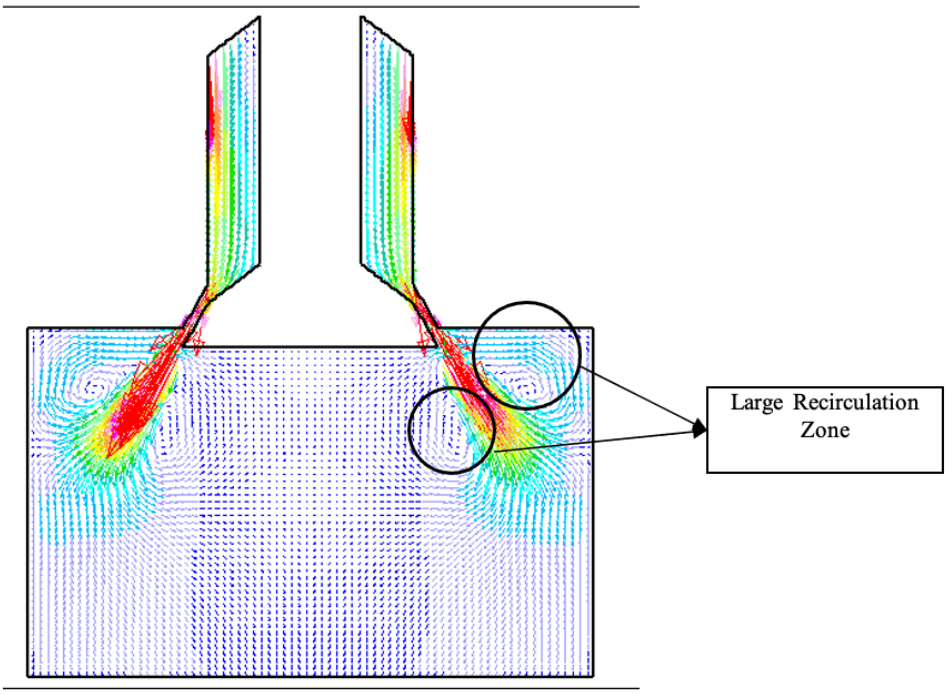

Figure 11. Velocity field predictions of *the k-*□ and RNG turbulence *model* for test Case I (□=36^{0}CA)

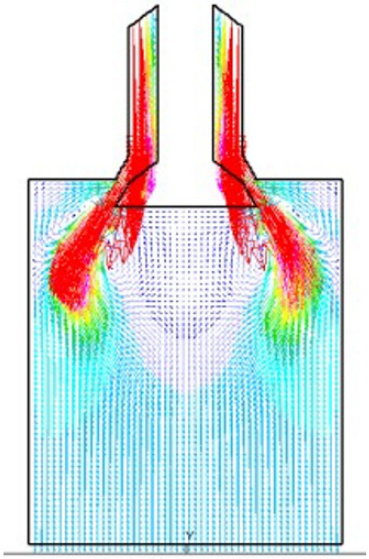

Figure 12. Velocity field predictions of *the k-□* and RNG turbulence *model* for test Case I at various crank angles in velocity contours and vector plots (□=90^{0}CA)

The predicted and measured tangential velocity and turbulence kinetic energy of the mean value for the whole cycle are shown in Figure 12. However at early stages as CA=360 and 900 there is a better match between measured results. For turbulence kinetic energy, the predictions are much lower than the measured values in the region below the valves. At 15mm below the cylinder head the predicted flow structure is very similar to that of the laser sheet images as seen in Figure 12.

Two cases are performed with k-e and RNG turbulence model. The main differences noted for the RNG k-eturbulence model were slightly better resolution of recirculation zones and a merging of the large and small vortices at 15mm below the cylinder head into one large vortex. Comparisons of both models with the LDA Measurements indicate that the tangential velocity predictions are better for the k-e model and the turbulence kinetic energy predictions are better with the RNG k-e model, especially at early stages of induction . Overall, there was no significant benefit in using the RNG k-e model in preference to the k-e model and subsequent simulations retained the k-e model. During early intake stroke the turbulence intensity contours of Figure 12 suggest that the origin of induction generated turbulence lies mainly within the shear layers on

either side of the induction jet. Turbulence intensity contours have higher gradients at the centers of the recirculation zones and impingement points on the cylinder wall. Turbulence is then transported downstream towards the piston but its diffusion towards the cylinder axis is small, resulting in low levels of turbulence in the region of the valve wake.

5. COMPARISON OF RESULTS WITH THE EXPERIMENTAL DATA

Comparison of results with the experimental data will give more accurate assessment of suggested turbulence model. It was done by comparing the predictions of the normalized mean axial velocity of the k-e models, and RNG model, with the measurements. Figures 13-15 show these comparisons between RNG, k-e turbulence model and measurement values.

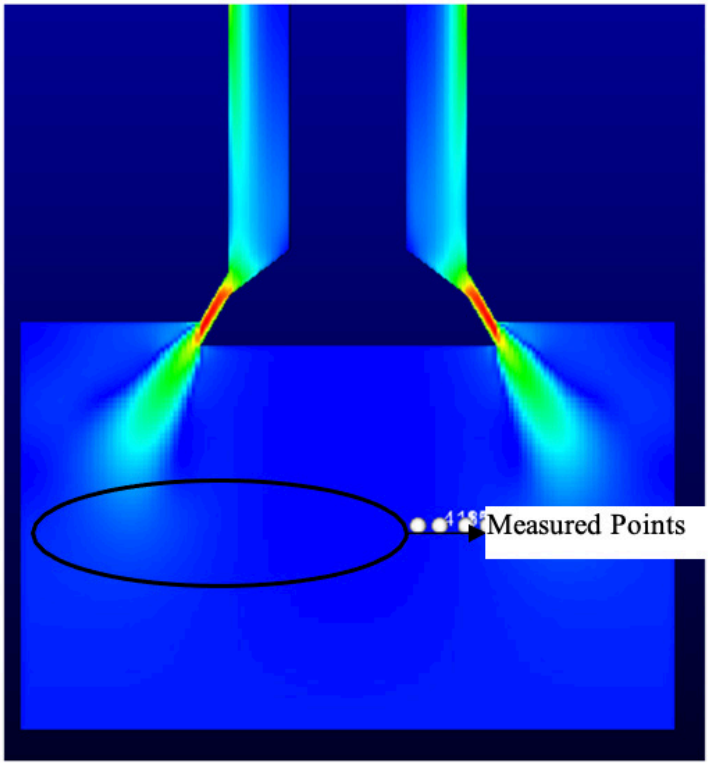

Figure 13. The comparison location z=15 mm for the two turbulence model

The measured and predicted radial profiles of the axial mean velocity and turbulence intensity at 36o are shown in Figure 14. The position of the peak in the radial velocity is well predicted by the k-□ and RNG model.

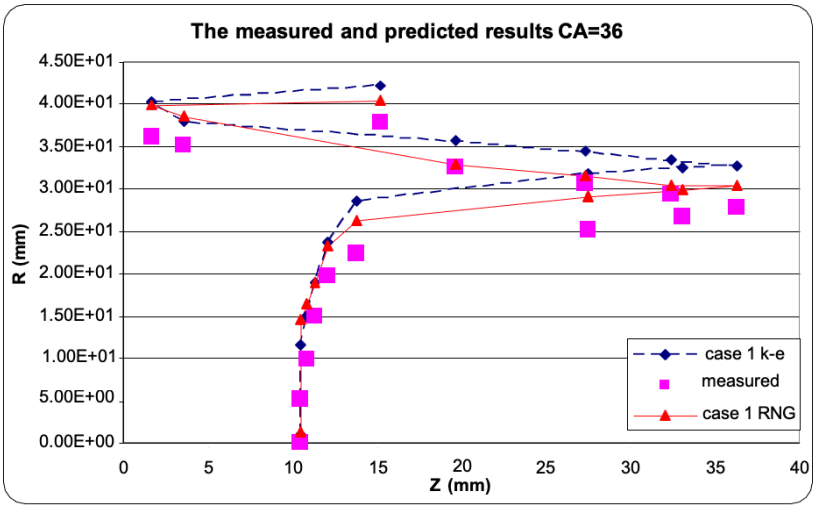

Figure 14. Comparison of Two Turbulence Model (□=36^{0}CA)

The comparisons of corresponding profiles at 90o are shown in Figure 15. The stretching of the main vortex by the piston and an increase in its peak velocity together with an increase in the level of turbulence intensity are evident from Figure 15. The predictions of both models show similar trends. However, the positions of the peak velocities and their magnitude as well as the recirculation zone behind the valve are captured well by the RNG model than the k-□ model. Turbulence intensities are also predicted better by the RNG model

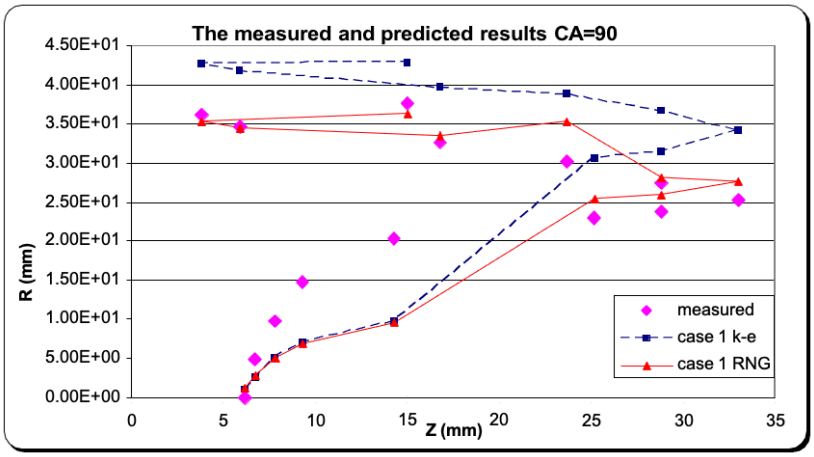

Figure 15. Comparison of two turbulence model for (□=90^{0}CA)

In Figure 15 the prediction of the mean velocity profiles at 270o shows that the strength of the main vortex persisting from the induction is grossly over-predicted by both turbulence models. According to data, the mean flow at the measurement location (z=15mm) is almost one dimensional, in the direction of the piston motion, except for a weak vortex near the cylinder wall and the turbulence intensity has decayed to the level 0.75 times of piston mean velocity and is virtually homogeneous. For the turbulence intensities, the RNG model and the MM k-□ model show an over prediction, although the tendency towards homogeneity is well predicted.

6. CONCLUSION

A series of transient flow simulations have been performed for axsymmetry engine configurations for valve lifts. The simulations were conducted on computational meshes constructed by an automatic meshing procedure that is included events and reordering vertices. This procedure delivers a mesh in less than 15% of the time required by current meshing techniques.

In this study, effects of the two different turbulence model for in-cylinder engine flows are obtained and compare the general performance during induction and compression stroke of the engine simulator. The predicted flow structure, in-cylinder tangential velocity and turbulence were compared LDA velocity and turbulence measurements. The following conclusions are drawn from the comparison. Good qualitative and quantitative agreement between the predicted and measured in-cylinder flow was obtained for full strokes. Both the RNG and the k-□-models yield qualitatively similar behavior of the in-cylinder flow, but the RNG model produces better profiles in most of the locations where comparisons are made with the experimental data.

In the majority of cases the predicted in-cylinder turbulence levels were significantly lower than the measured values. Switching to an RNG k-e turbulence model resulted in only a minor improvement in the predicted turbulence levels. Because the RNG model damps main vortex more, giving better agreement for the mean velocities than the k-model during late compression stroke. Predicted turbulence intensities by the the k-□ model during this stage are in good agreement with the data.

REFERENCES

[1] W. Shyy, S.S.T., Computational Techniques for complex transported phenomena. New York, Cambridge, (1997)100-115

[2] Shyy W, U.H., Computational Fluid Dynamics with Moving Boundaries. Taylor and Francis, Washington DC. (1996) 116-125.

[3] Gul, M.Z.: "Prediction of In-Cylinder Flow by Use of a Multiple-Time-Scale Turbulence Model", PhD Thesis, Victory University of Manchester, (1994) 60-90.

[4] Wu, C.T., Ferziger, J.H; Chapman, D.R., Simulation and modeling of homogeneous, compressed turbulence. Fifth Symp. of Turbulent Shear Flows, Cornell Univ, (1985) 17.13-17.20.

[5] Hergart, C., Barths, H., and Peters, N., Modeling the Combustion Process in a Small-Bore Diesel Engine Using a Model Based on Representative Interactive Flamelets. SAE Technical Paper Series, (1999) 1999-01-3550.

[6] P., M., In-Cylinder Turbulent Flow Structure in Direct Injection, Swirl Supported Diesel Engines. (2003)

[7] Zhang, Y., A Numerical Study of In-Cylinder Mixture Formation in a Low Pressure Direct Injection Gasoline Engine, in Master Degree of Science. Michigan State University. (2007)

[8] Haworth, Multidimensional port-and-cylinder flow calculations for two and four valve-per-cylinder engines: influence of intake configuration on flow structure. SAE Technical Paper Series, (1990) p. 647-678.

[9] Heywood, J.B., Fluid motion within the cylinder of internal combustion engines- the 1986 freeman scholar lecture. . Journal of Fluids Engineering, (1987). 109: p. 3-35.

[10] Davis, G.C., Mikulec, A., Kent, Modeling the Effect of Swirl on Turbulence Intensity and Burn Rate in S.I.Engines and Comparison with Experiment. SAE Technical Paper Series, (1986)

[11] Witze, P.O., The Effect of Spark Location in Combustion in a Variable

Swirl Engines. SAE Technical Paper Series, (1982) 820044.

[12] Nagayama, I., Araki, Y., and Ioka, Y, Effects of Swirl and Squish on S.I. Engine Combustion and Emission. SAE Technical Paper Series, (1977)

[13] Drake M.C., H.D., Advanced gasoline engine development using optical diagnostics and numerical modeling Proceedings of a Symposium on Combustion (2007)

[14] Moureau V., B.I., Towards Large Eddy Simulation in ICE: simulations of a compressed tumble flow. SAE Technical Paper Series, (1994)

[15] Launder B.E., S., D.B., Mathematical Models of Turbulence. New York, Academic Press, (1972)